Signature of nearly icosahedral structures in liquid and supercooled liquid copper

P. Ganesh and M. Widom
Department of Physics, Carnegie Mellon University, Pittsburgh, Pennsylvania 15213, USA
(Received 9 February 2006; revised manuscript received 26 July 2006; published 30 October 2006)

A growing body of experiments display indirect evidence of icosahedral structures in supercooled liquid metals. Computer simulations provide more direct evidence but generally rely on approximate interatomic potentials of unproven accuracy. We use first-principles molecular dynamics simulations to generate realistic atomic configurations, providing structural detail not directly available from experiment, based on interatomic forces that are more reliable than conventional simulations. We analyze liquid copper, for which recent experimental results are available for comparison, to quantify the degree of local icosahedral and polytetrahedral order.

DOI: 10.1103/PhysRevB.74.134205 PACS number(s): 61.25.Mv, 61.43.Dq, 61.20.Ja, 71.15.Pd

I. INTRODUCTION

Turnbull[1–3] established that metallic liquids can be supercooled if heterogeneous nucleation can be reduced or avoided. Later, Frank hypothesized that the supercooling of liquid metals might be due to frustrated packing of icosahedral clusters. Icosahedral clustering of 12 atoms about a sphere is energetically preferred to crystalline (e.g., fcc, hcp or bcc) packings for the Lennard-Jones (LJ) pair potentials. The icosahedron is favorable because it is made up entirely of four-atom tetrahedra, the densest-packed cluster possible. Local icosahedral order cannot be propagated throughout space without introducing defects.

Remarkably, the frustration of packing icosahedra is relieved in a curved space, where a perfect 12-coordinated icosahedral packing exists.[4–6] Disclination line defects must be introduced into this icosahedral crystal in order to "flatten" the structure and embed it in ordinary three-dimensional space. Owing to the five-fold rotational symmetry of an icosahedron, the disclination lines are of type 72°. The negative disclination line defects that are needed to flatten the structure cause increased coordination numbers of 14, 15 or 16. Large atoms, if present, would naturally assume high coordination number and aid in the formation of a disclination line network.

Many studies of Lennard-Jones systems have tested Frank's hypothesis. Hoare[7] found that for clusters ranging between 2 to 64 atoms at least three types of "polytetrahedral" noncrystalline structures exist, with a higher binding energy than hcp or fcc structures with the same number of atoms. Honeycutt and Andersen[8] found the crossover cluster size between icosahedral and crystallographic ordering around a cluster size of 5000 atoms. They also introduced a method to count the number of tetrahedra surrounding an interatomic bond. This number is 5 for local icosahedral order. Steinhardt, Nelson, and Ronchetti[9] introduced the orientational order parameter $\hat{W}_6$ to demonstrate short range icosahedral order.

Many other simulations have been performed on pure elemental metals and metal alloys, using a modified Johnson potential,[10] embedded atom potentials,[11,12] the Sutton-Chen (SC) many-body potential,[13] to name a few. These potentials model the interatomic interactions with varying, and generally uncontrolled, degrees of accuracy. *Ab initio* studies on liquid copper,[14,15] aluminum,[16] and iron[17] achieve a high degree of realism and accuracy, but have not been analyzed from the perspective of icosahedral ordering. Nevertheless, recent *ab initio* studies on Ni and Zr (Refs. 18 and 19) have been done with this perspective and find that with supercooling the degree of icosahedral ordering increases in Ni while in Zr bcc is more favored.

X-ray diffraction measurements of electrostatically levitated droplets of Ni (Ref. 20) found evidence of distorted icosahedral short ranged order. Neutron scattering studies of deeply undercooled metallic melts[21] observed the characteristic shoulder on the second peak of the structure factor, which has been identified as a signature of icosahedral short range order.[22,23] The shoulder height increases with decrease in temperature.

A recent XAS (x-ray absorption spectroscopy) experiment on liquid and undercooled liquid Cu by Di Cicco *et al.*[24] isolated the higher order correlation functions. They applied reverse Monte Carlo (RMC) refinement[25–27] simultaneously to diffraction and XAS data to construct a model of the disordered system compatible with their experimental data. They analyze the three-body angular distribution function $N(\theta)$ and also the orientational order parameter $\hat{W}_6$. Their conclusion was that weak local icosahedral order could be observed in their sample. This experiment provided the most direct experimental evidence to date of the existence of icosahedra in a liquid metal.

Motivated by these results, we explore the structures of liquid and undercooled liquid metals using first principles simulations. First principles calculations achieve the most realistic possible structures, unhindered by the intrinsic inaccuracy of phenomenological potentials, and with the ability to accurately capture the chemical nature and distinctions between different elements and alloys. We use the VASP (Vienna *ab initio* simulation package[28,29]) code which solves the quantum mechanical interacting many-body problem using electronic density functional theory. These forces are incorporated into a molecular dynamics simulation. The tradeoff for increased accuracy is a decrease in the system sizes we can study, so we can only observe local order, not long range. Also we are limited to short time scales.

Our analysis covers methods that have previously been fruitful. We look at the radial distribution function, the struc-

ture factor, the three-body angular distribution function, which is simply related to the three-body correlation function, the $\hat{W}_6$ parameter as discussed above, and the Honeycutt and Andersen bond statistics method.[8]

The extent of the icosahedral order that we observe in simulation is qualitatively in agreement with recent experiments.[24] At high temperatures we found that structural properties of liquid Cu strongly resembled a maximally random jammed[30] hard sphere configuration. From this we conclude that a nearly universal structure exists for single component systems whose energetics are dominated by repulsive central forces. The degree of icosahedral order is not great, presumably due to the frustration of icosahedra, but it does show a tendency to increase as temperature drops.

Section II describes our first principles molecular dynamics method in greater detail. The next section, Sec. III discusses our study on copper. Here we introduce the radial distribution function $g(r)$, the liquid structure factor $S(q)$, the $\hat{W}_6$ bond orientational order parameter, the three-body angular distribution function $N(\theta)$, and the Honeycutt and Andersen analysis method. We conclude, in Sec. IV, with some thoughts about enhancing icosahedral order by alloying with a fraction of smaller and larger atoms.

II. FIRST PRINCIPLES METHOD

First principles simulation is an incisive, powerful and well-developed tool based on a quantum mechanical treatment of the electrons responsible for interatomic bonding. Since the method is based on fundamental physical laws and properties of atoms, it can be applied to a wide variety of metals, including alloys, and yields the energy and forces computationally without any adjustable free parameters.

Our *ab initio* molecular dynamics simulation program, VASP,[28,29] solves the N-body quantum mechanical interacting electron problem using electronic density functional theory, under the generalized gradient approximation (GGA). We use the projector-augmented wave[31,32] (PAW) potentials as provided with VASP. Calculation times grow nearly as the third power of the number of atoms, limiting our studies to sample sizes of around 100 atoms.

In first-principles molecular dynamics, although interatomic forces and energies are calculated quantum mechanically, we still treat the atomic motions classically, using the Born-Oppenheimer approximation. We use Nose dynamics[33] to simulate in the canonical ensemble at fixed mean temperature. The system was well equilibrated before data was considered for analysis. The simulation started with a random configuration, at a temperature high enough to ensure a liquid state, and was allowed to equilibrate at this high temperature. Subsequently, lower temperatures were simulated starting from previous configurations. All calculations were Γ point calculations (a single k point).

We took $N=100$ Cu atoms and applied periodic boundary conditions in an orthorhombic cell. Our unequal lattice parameters avoid imposing a characteristic length on the system. The simulations were done at three different temperatures, $T=1623$ K, 1398 K, and 1313 K in order to compare with Di Cicco's experiments.[24] The melting point of copper is $T=1356$ K, so samples at 1623 K and 1398 K are in the liquid regime, while the one at 1313 K is undercooled. We used number densities of 0.0740 Å^{-3}, 0.0758 Å^{-3}, and 0.0764 Å^{-3}, respectively, at $T=1623$ K, 1398 K, and 1313 K. These were obtained from a fit of the XRD experimental volume per particle[34] to a straight line versus temperature. Starting from configurations that had been previously equilibrated at slightly different densities, transients of about 250 steps (1 fs per step) passed prior to the onset of equilibrium fluctuations of the energy. After the transient, a total of 3000 MD steps were taken at each temperature, for a total simulation time of 3 ps. The run time was around 480 h on a 2.8 GHz Intel Xeon processor for each temperature. Subsequently, two configurations from the highest temperature run, widely separated in time, were selected and used as the starting configuration for two runs at $T=1398$ K, with proper scaling of densities. After an initial transient of 250 steps, these runs were further continued at $T=1313$ K as well as at $T=1398$ K. The four runs, two at $T=1398$ K and two at $T=1313$ K were carried on for 1 ps, during which time the energy showed equilibrium fluctuations. All of these runs have been used for analyzing the local order in liquid copper.

For a few selected configurations, a conjugate-gradient algorithm was used to relax the ions to their instantaneous ground state, to explore their inherent structures.[35] Surprisingly all of our samples partially crystallized, based on visual observation. Further efforts to obtain quenched amorphous structures used steepest-descent minimization and molecular dynamics with a linear temperature ramp, followed by steepest-descent minimization. Again the structures partially crystallized. There appear to be no fully amorphous relaxed structures accessible for Cu using these methods.

III. RESULTS

A. Radial distribution function $g(r)$

The radial distribution function, $g(r)$, is proportional to the density of atoms at a distance r from another atom. We calculate $g(r)$ by forming a histogram of bond lengths. We use the repeated image method to obtain bond lengths greater than one-half the box size, and anticipate $g(r)$ in this range may be strongly influenced by finite size effects. We then smooth out with a Gaussian of standard deviation 0.05 Å. Figure 1 shows the $g(r)$ we obtained at the three different temperatures. Our $g(r)$ at $T=1623$ K, compares well with $g(r)$ interpolated from XRD experiments,[34] with the two curves overlapping almost everywhere except for a small disagreement in the position of the first peak. Results from neutron diffraction experiment[36] at $T=1393$ K, compare well with our $g(r)$ at $T=1398$ K. Comparisons with the $g(r)$ for Cu at 1500 K from the *ab initio* MD studies by Hafner *et al.*[15] and Vanderbilt *et al.*[14] finds that the heights of their first peak match well with our $g(r)$ (interpolated to $T=1500$ K). But their peak positions are shifted slightly to the left of ours (ours is at 2.50 Å). The $g(r)$ from an embedded-atom method (EAM) model for Cu[12] which matches almost exactly with the XRD data at $T=1773$ K, is also consistent with our extrapolated $g(r)$ at this temperature.

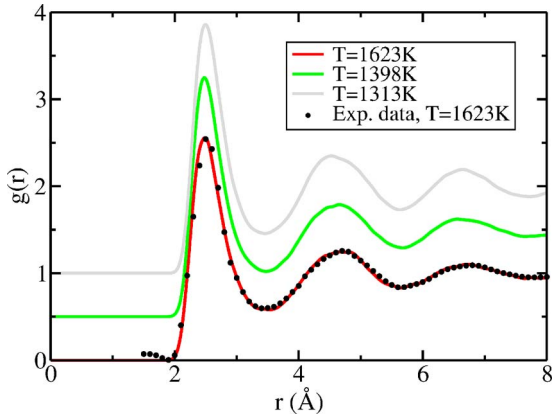

FIG. 1. (Color online) Simulated liquid Cu radial distribution function, $g(r)$, at three different temperatures. The simulated curve at $T=1623$ K matches well with the experimental XRD (x-ray diffraction) result (Ref. 34) interpolated to $T=1623$ K. [The simulated $g(r)$ at $T=1313$ K and $T=1398$ K have been shifted up for visual clarity.]

The growth in height of the peaks in the supercooled system at $T=1313$ K suggests an increase of some type of order. However this order is not related to the crystalline fcc equilibrium phase, as we show in the following sections.

To test for finite size effects in our $N=100$ atom system, we ran a separate simulation for $N=200$ atoms at the intermediate temperature $T=1398$ K (Fig. 2). The first and second peaks of $g(r)$ for both the system sizes compare very well. There is a small but significant difference in the depth of the first minimum, then systematic differences between the curves beyond 5 Å. From this we conclude that the finite size effect is not important at small r values, but for larger values of r (beyond 5 Å) there is a weak finite size effect. The three-body angular distributions, and the $\hat{W}_6$ histograms of the $N=200$ and the $N=100$ runs, are also comparable, suggesting that $N=100$ is sufficient for studies of local order of the types we consider here.

We calculate the coordination number from the radial distribution function $g(r)$. We choose a cutoff distance near the first minimum of $g(r)$, at $R_{\text{cut}}=3.4$ Å. The precise location of the minimum is difficult, and its variation with temperature is smaller than the error in locating its position (Fig. 1), so that we do not change the value of R_{cut} with temperature. With this value of R_{cut} we find an average coordination number (N_c) of 12.3 which is nearly independent of temperature (N_c changes from 12.1 at high temperature to 12.5 with supercooling). However, our range of evolution of N_c is small compared to the case of Ni,[18] since our degree of supercooling is much lower (3%) than theirs (17%). We are not able to achieve a higher degree of supercooling of Cu as mentioned earlier in the paper.

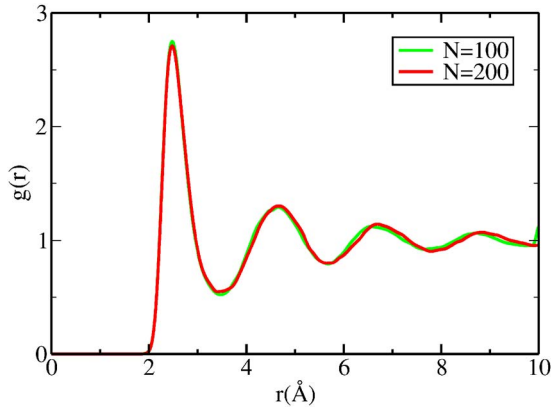

FIG. 2. (Color online) Simulated liquid Cu radial distribution function, $g(r)$, at $T=1398$ K for $N=100$ and $N=200$ atoms. A weak finite size effect is observed after about $r=5$ Å.

B. Liquid structure factor $S(q)$

The liquid structure factor $S(q)$ is related to the radial distribution function $g(r)$ of a liquid with density ρ by

$$S(q) = 1 + 4\pi\rho \int_0^\infty [g(r) - 1] \frac{\sin(qr)}{qr} r^2 dr. \tag{1}$$

Evidently, one needs a knowledge of the radial distribution function up to large values of r to get a good $S(q)$. In our first principles simulation, we are restricted to small values of r, due to our small system sizes, so we need a method to get $S(q)$ from our limited range $g(r)$ function.

Baxter developed a method[37,38] to extend $g(r)$ beyond the size of the simulation cell. The method exploits the short ranged nature of the direct correlation function $c(r)$, which has a range similar to the interatomic interactions,[39] as opposed to the $g(r)$ which is much long ranged. The exact relation that connects these two functions is the Ornstein-Zernike relation,

$$h(r) = c(r) + \rho \int h(|\mathbf{r} - \mathbf{r}'|) c(|\mathbf{r}'|) d\mathbf{r}', \tag{2}$$

where $h(r)=g(r)-1$.

Assuming that $c(r)$ vanishes beyond a certain cutoff distance r_c, Baxter obtained a pair of equations, valid for $r < r_c$. The remarkable property of this method is that if we know $h(r)$ over a range $0 \leqslant r \leqslant r_c$, then we can obtain $c(r)$ over its entire range (from 0 to r_c), which implicitly determines $h(r)$ over its entire range (from 0 to ∞) through Eq. (2).

We solve the Baxter's equations iteratively to obtain the full direct correlation function. A complete knowledge of the direct correlation function gives us the structure factor $S(q)$ in terms of its Fourier transform $\hat{c}(q)$,

$$S(q) = \frac{1}{1 - \rho \hat{c}(q)}, \tag{3}$$

where

$$\hat{c}(q) = 4\pi \int_0^\infty r^2 c(r) \frac{\sin(qr)}{qr} dr. \tag{4}$$

The $S(q)$ showed good convergence with different choices of r_c, and a choice of $r_c=5$ Å seemed appropriate because it was one-half of our smallest simulation cell edge length.

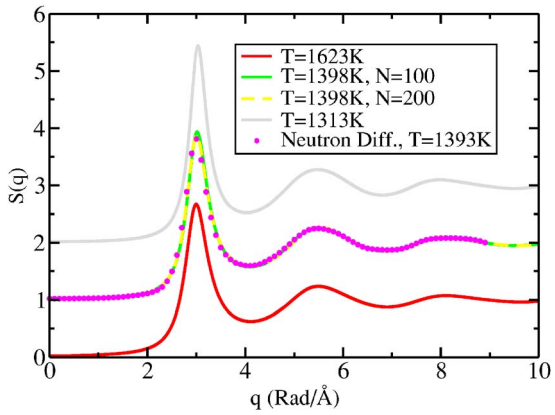

FIG. 3. (Color online) Liquid structure factor $S(q)$ as obtained from the simulated radial distribution function $g(r)$ at $T=1398$ K compared with the $S(q)$ from neutron diffraction at $T=1393$ K (Ref. 36). The calculated $S(q)$ at the other two temperatures are also plotted, and show the expected temperature behavior. [The $S(q)$ at $T=1313$ K and $T=1398$ K have been shifted up for visual clarity.]

Even though in metals there are long range oscillatory Friedel oscillations, our ability to truncate $c(r)$ at $r_c=5$ Å, shows that these are weak compared with short range interactions.

Figure 3 compares the calculated $S(q)$ at our three different temperatures, and the experimental neutron $S(q)$ at $T=1393$ K.[36] The calculated $S(q)$ at $T=1398$ K compares well with the experiment at all values of q. The $S(q)$ from the larger system is in better agreement with the experiment. Comparison between the two system sizes suggest again that the finite size effects are significant but not important, and $N=100$ is good enough to get a representative liquid structure. No resolution correction was applied to the experimental data, and moreover it was smoothed. Both of these cause a decrease in the height of the actual $S(q)$, which becomes quite appreciable at the first peak. As a test, we also applied a resolution correction to our simulated $S(q)$ (not shown), which reduced the height of the first peak bringing it in closer agreement with the experimental value. Nevertheless the overall excellent agreement shows that the first principles simulation with only $N=100$ atoms is able to produce representative structures at $T=1398$ K. This enables us to make further studies of the local icosahedral and polytetrahedral order in liquid and supercooled liquid copper.

As mentioned earlier in the introduction, one signature of icosahedral short range order is the splitting of the second peak of $S(q)$.[22,23] Even though we observe weak icosahedral order in Cu (discussed later in this paper), we do not observe a clear splitting of the second peak in $S(q)$ (Fig. 3), but we do observe a broadening as we lower the temperature. We think that the absence of splitting could be because of our low degree of supercooling.

C. Bond orientation order parameters

As introduced by Steinhardt *et al.*,[9] the $\hat{W}_l$ parameters are a measure of the local orientational order in liquids and undercooled liquids. To calculate $\hat{W}_l$, the orientations of bonds from an atom to its neighboring atoms are projected onto a basis of spherical harmonics. Rotationally invariant combinations of coefficients in the spherical harmonics expansion are then averaged over many atoms in an ensemble of configurations. The resulting measures of local orientational order can be used as order parameters to characterize the liquid structures. For an ideal icosahedral cluster, $l=6$ is the minimum value of l for which $\hat{W}_6 \neq 0$. Table I enumerates $\hat{W}_6$ values for different ideal clusters. We see that the ideal icosahedral value of $\hat{W}_6$ is far from other clusters, making it a good icosahedral order indicator.

TABLE I. $\hat{W}_6$ values for a few clusters.

Cluster	hcp	fcc	icos	bcc
Number of atoms	12	12	12	14
$\hat{W}_6$	−0.012	−0.013	−0.169	+0.013

We choose the cutoff distance to specify near neighbors at $R_{\text{cut}}=3.4$ Å as before. Our value of R_{cut} is significantly greater than that of Di Cicco *et al.* Our $\hat{W}_6$ distributions (Fig. 4) show strong asymmetry favoring negative values with tails extending towards the ideal icosahedron value. Because the histogram vanishes as $\hat{W}_6$ approaches its limiting negative value we see that there are essentially no perfectly symmetric undistorted icosahedra present in our simulation. However, a significant fraction do have $\hat{W}_6$ values close to the icosahedral value.

A $\hat{W}_6$ analysis was performed for a 10^4 atom maximally random jammed hard sphere configuration.[30] The diameter of the hard spheres was rescaled so that the position of the main peak of the resulting $g(r)$ matched the value $r=2.5$ Å found for Cu at $T=1623$ K. The R_{cut} value for the MRJ configuration was taken near the first minimum of the $g(r)$ at $r=3.3$ Å. Remarkably, the $\hat{W}_6$ distribution of the MRJ configuration (Fig. 4) is similar to the distribution for liquid Cu at high temperature, suggesting that the structure of Cu under this condition is dominated by strongly repulsive short-range central forces.

As we lower the temperature of liquid Cu, the mean value of $\hat{W}_6$ drops and the peak of the $\hat{W}_6$ distribution shifts to the

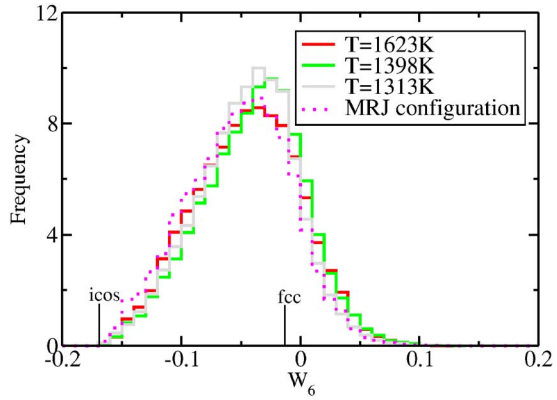

FIG. 4. (Color online) Simulated $\hat{W}_6$ distributions for liquid Cu. Ideal icosahedron and fcc values are indicated.

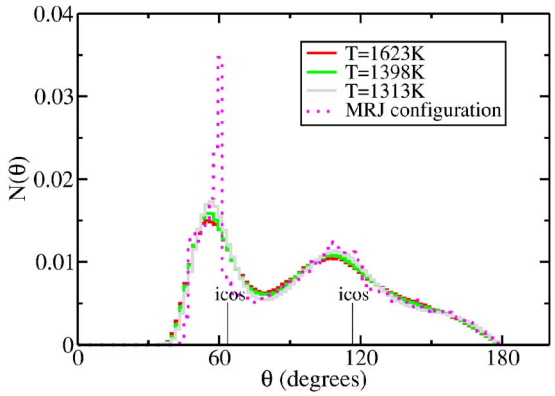

FIG. 5. (Color online) Distribution of $N(\theta)$ for liquid Cu. Ideal icosahedron values are indicated.

left. However, the peak never moves below $\hat{W}_6 = -0.05$, and the tail of the distribution at negative $\hat{W}_6$ shows no strong temperature dependence. It seems that there is no change in the number of nearly icosahedral clusters as the temperature drops into the supercooled regime, possibly a result of the frustration of icosahedral packing. Our liquid has a single component, so there is no natural way to introduce disclinations. This inhibits the growth of a population of atoms with $\hat{W}_6$ close to its ideal icosahedral value.

Comparing our result with that of Di Cicco *et al.* at $T = 1313$ K, we see that our curve is more asymmetric towards negative values than Di Cicco's, so that we see a greater fraction of atoms near the ideal icosahedral value of $\hat{W}_6$. The discrepancy probably lies in the difference between the two methods used to generate the positional configurations (the difference is even greater if we use Di Cicco's value of R_{cut}). Their configurations were obtained using reverse Monte Carlo (RMC), which does not guarantee accurate configurations. Our first principles method should be more accurate in determining these configurations. Of course, Di Cicco's configurations *are* consistent with experimentally measured three-body correlations. It would be of great interest to see if our configurations are also consistent with the raw experimental data. The differences in $\hat{W}_6$ distributions should not be overstated—the experiment and our simulations both show that liquid and supercooled liquid copper has weak but non-negligible icosahedral order.

D. Bond angle distribution $N(\theta)$

The bond angle distribution $N(\theta)$ is a simple type of three-body correlation function. Let θ be the angle between bonds from a single atom to two neighbors, and define $N(\theta)$ as the probability density for angle θ, normalized such that the total probability, $\int N(\theta) d\theta = 1$. The distribution for the central atom of an ideal 13-atom icosahedral cluster, shows peaks at 63.4°, 116.4°, and 180.0°. For other crystallographic clusters, like hcp, fcc, and bcc, we see peaks at 60°, 90°, and 120°. Angles around 60° indicate nearly equilateral triangles that may well belong to tetrahedra.

Figure 5 shows the distributions for copper at three temperatures. We have chosen the same value of R_{cut} that was used to obtain $\hat{W}_6$ in Sec. III C. The distribution function shows maxima at 56° and 110° with a minimum around 80°. Our result is similar to that of Di Cicco (they show only $T = 1313$ K), but with more pronounced minimum and second maximum. The peak around 60° shows an abundance of nearly equilateral triangles, indicating the presence of tetrahedrons, which can pack to form icosahedra. The minimum close to 90° shows that there are not many cubic clusters. We also see that the high-angle tail at high temperature turns into a broad maximum at low temperature centered around 165°. This may represent a shifting of the ideal 180° peak caused by cluster distortion. The ordering increases as temperature decreases, indicating that the number of nearly equilateral triangles increases when the liquid is undercooled, probably caused by an increase in polytetrahedral order with undercooling.

The distribution of the MRJ configurations (same R_{cut} as defined in Sec. III C) shows a sharp peak at exactly 60°, a broad peak at 110° and a minimum around 90°. The peak at 60° shows an overwhelming presence of perfectly equilateral triangular faces, which are easily formed when three hard spheres come in contact with each other. But the minimum around 90° and a second maximum nearer to 110° as opposed to 120°, suggests that the local order is not fcc or hcp. This feature of the MRJ configuration agrees qualitatively with the angular distribution of liquids, implying an underlying universal structure for systems whose energetics are dominated by repulsive central forces. But the quantitative differences also emphasize the necessity to exactly model an atomic liquid to study its local environments, and quantify polytetrahedral order.

E. Honeycutt and Andersen analysis

Honeycutt and Andersen[8] introduced a useful assessment of local structure surrounding interatomic bonds. We employ a simplified form of their analysis, counting the number of common neighbors shared by a pair of near-neighbor atoms. This identifies the number of atoms surrounding the near-neighbor bond and usually equals the number of edge-sharing tetrahedra whose common edge is the near-neighbor bond. We assign a set of three indices to each bond. The first index is 1 if the root pairs are bonded (separation less than or equal to R_{cut}). The second index is the number of near-neighbor atoms common to the root pairs, and the third index gives the number of near-neighbor bonds between these common neighbors. We take $R_{\text{cut}} = 3.4$ Å as before. Note that the Honeycutt and Andersen fractions depend sensitively on R_{cut}, making precise quantitative comparisons with other prior studies difficult.

In general, 142's are characteristic of close packed structures (fcc and hcp) and 143's are characteristic of distorted icosahedras.[40] They can also be considered as +72° disclinations.[4–6] Likewise, 15's are characteristic of icosahedra, and 16's indicate −72° disclinations. Figure 6 shows the 14's, 15's, and 16's for liquid Cu at the three temperatures. The error bars shown were calculated by breaking the data into three subsets. The 14's have been separated into 142's

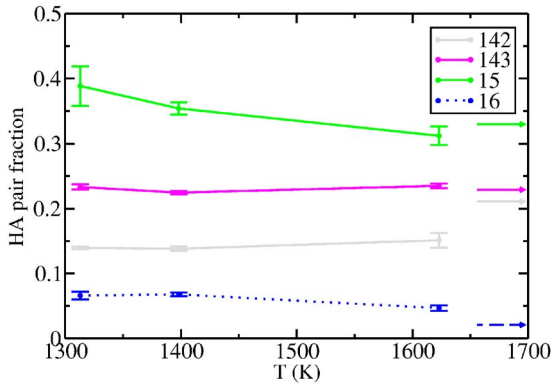

FIG. 6. (Color online) Honeycutt-Andersen pair fractions for 142's (fcc and hcp forming +72° disclination), 15's (icosahedron), and 16's (−72° disclination) at different temperatures. The increase in 15's as temperature is reduced show increased icosahedral ordering with supercooling. The corresponding HA values for the MRJ configurations are indicated on the right-hand side of the plot.

and 143's. The remaining 14's are mostly 144's with fraction around 0.04. The fraction of 142's and 143's holds steady with temperature, with the icosahedral fraction always exceeding the close packed fraction. As the temperature drops, the fraction of 15's grows. At each of the three temperatures, the 15's are mainly comprised of 154's (characteristic of distorted icosahedra) and 155's (characteristic of perfect icosahedra), with the 154's slightly higher than the 155's. Of all the 16's, the 166's are the highest and steadily increase with lowering of temperature. The 166's indicate the −72° disclination lines, which relieve the frustration of icosahedral order.

These trends indicate a weak increase in polytetrahedral ordering with supercooling. The same trend was observed in simulations based on Sutton-Chen potentials[13] except for the fact that our 142's are slightly higher compared to their 142's.

For comparison, the values for a maximally random jammed packing[30] (R_{cut}=3.3 Å) are shown in Fig. 6. These values are fairly close to liquid Cu at high temperature, and also to a similar common neighbor analysis of dense random-packing of hard spheres.[41] These results are consistent with our previous observation for the $\hat{W}_6$ distribution and $N(\theta)$, that a nearly universal structure arises at high temperature, dominated by repulsive central forces.

IV. CONCLUSION

This study quantifies icosahedral and polytetrahedral order in supercooled liquid copper. While the structural properties of high temperature liquid Cu are close to a maximally random jammed structure,[30] proper modeling of atomic interactions is essential to capture the behavior of an element at liquid and supercooled temperatures. A first-principles simulation is the most reliable means of achieving this. We find small but significant disagreement with analysis based on reverse Monte Carlo simulation.

Supercooled liquid copper shows a slight increase in icosahedral and polytetrahedral order as temperature drops, which is consistent with recent experiments.[20,21,24] The frustration of icosahedrons in the one component liquid inhibits formation of perfect icosahedra, giving rise to defective icosahedrons. Alloying with larger atoms might relieve the frustration of packing icosahedrons by encouraging the formation of −72° disclinations.[42,43] Alloying with smaller atoms can relieve frustration of individual icosahedrons by placing the smaller atom at the center.[44] Alloying with larger and smaller atoms simultaneously thus offers the chance to optimize icosahedral order. Work is in progress in achieving the same.[45]

ACKNOWLEDGMENTS

This work was supported in part by Grant No. NSF/DMR-0111198. The authors thank Sal Torquato for providing maximally random jammed configurations of hard spheres.

[1] D. Turnbull, J. Appl. Phys. **21**, 1022 (1950).
[2] D. Turnbull, J. Met. **2**, 1144 (1950).
[3] D. Turnbull and R. E. Cech, J. Appl. Phys. **21**, 804 (1950).
[4] J. F. Sadoc and R. Mosseri, Philos. Mag. B **45**, 467 (1982).
[5] D. R. Nelson, Phys. Rev. Lett. **50**, 982 (1983).
[6] J. P. Sethna, Phys. Rev. Lett. **51**, 2198 (1983).
[7] M. R. Hoare, J. Cryst. Growth **17**, 77 (1972).
[8] J. D. Honeycutt and H. C. Andersen, J. Phys. Chem. **91**, 4950 (1987).
[9] P. J. Steinhardt, D. R. Nelson, and M. Ronchetti, Phys. Rev. B **28**, 784 (1983).
[10] T. Tomida and T. Egami, Phys. Rev. B **52**, 3290 (1995).
[11] C. Kuiying, L. Hongbo, L. Xiaoping, H. Quiyong, and H. Zhuangqi, J. Phys.: Condens. Matter **7**, 2379 (1995).
[12] B. Sadigh and G. Grimvall, Phys. Rev. B **54**, 15742 (1996).
[13] H. J. Lee, T. Cagin, W. L. Johnson, and W. A. Goddard, J. Chem. Phys. **119**, 9858 (2003).
[14] A. Pasquarello, K. Laasonen, R. Car, C. Lee, and D. Vanderbilt, Phys. Rev. Lett. **69**, 1982 (1992).
[15] G. Kresse and J. Hafner, Phys. Rev. B **48**, 13115 (1993).
[16] A. A. Valladares, J. Non-Cryst. Solids (to be published).
[17] D. Alfe, G. Kresse, and M. J. Gillan, Phys. Rev. B **61**, 132 (2000).
[18] N. Jakse and A. Pasturel, J. Chem. Phys. **120**, 6124 (2004).
[19] N. Jakse and A. Pasturel, Phys. Rev. Lett. **91**, 195501 (2003).
[20] G. W. Lee, A. K. Gangopadhyay, K. F. Kelton, R. W. Hyers, T. J. Rathz, J. R. Rogers, and D. S. Robinson, Phys. Rev. Lett. **93**, 037802 (2004).
[21] T. Schenk, D. Holland-Moritz, V. Simonet, R. Bellissent, and D. M. Herlach, Phys. Rev. Lett. **89**, 075507 (2002).
[22] D. R. Nelson and M. Widom, Nucl. Phys. B **240**, 113 (1984).
[23] S. Sachdev and D. R. Nelson, Phys. Rev. Lett. **53**, 1947 (1984).
[24] A. DiCicco, A. Trapananti, S. Faggioni, and A. Filipponi, Phys. Rev. Lett. **91**, 135505 (2003).

[25] R. L. McGreevy, J. Phys.: Condens. Matter **13**, R877 (2001).
[26] S. J. Gurman and R. L. McGreevy, J. Phys.: Condens. Matter **2**, 9463 (1990).
[27] Y. Wang, K. Lu, and C. Li, Phys. Rev. Lett. **79**, 3664 (1997).
[28] G. Kresse and J. Hafner, Phys. Rev. B **47**, R558 (1993).
[29] G. Kresse and J. Furthmuller, Phys. Rev. B **54**, 11169 (1996).
[30] S. Torquato, T. M. Truskett, and P. G. Debenedetti, Phys. Rev. Lett. **84**, 2064 (2000).
[31] P. E. Blochl, Phys. Rev. B **50**, 17953 (1994).
[32] G. Kresse and D. Joubert, Phys. Rev. B **59**, 1758 (1999).
[33] S. Nose, J. Chem. Phys. **81**, 511 (1984).
[34] Y. Waseda, *The Structure of Non-Crystalline Materials* (McGraw-Hill, New York, 1980).
[35] F. H. Stillinger and T. A. Weber, Phys. Rev. A **25**, 978 (1982).
[36] O. J. Eder, E. Erdpresser, B. Kunsch, H. Stiller, and M. Suda, J. Phys. F: Met. Phys. **10**, 183 (1980).
[37] R. J. Baxter, J. Chem. Phys. **52**, 4559 (1970).
[38] D. J. Jolly, B. C. Freasier, and R. J. Bearman, Chem. Phys. **15**, 237 (1976).
[39] S. M. Foiles and N. W. Ashcroft, J. Chem. Phys. **81**, 6140 (1984).
[40] W. K. Luo, H. W. Sheng, F. M. Alamgir, J. M. Bai, J. H. He, and E. Ma, Phys. Rev. Lett. **92**, 145502 (2004).
[41] A. S. Clarke and H. Jonsson, Phys. Rev. E **47**, 3975 (1993).
[42] N. Jakse, O. Lebacq, and A. Pasturel, Phys. Rev. Lett. **93**, 207801 (2004).
[43] N. Jakse, O. Lebacq, and A. Pasturel, J. Chem. Phys. **123**, 104508 (2005).
[44] H. W. Sheng, W. K. Luo, F. M. Alamgir, J. M. Bai, and E. Ma, Nature (London) **439**, 419 (2006).
[45] P. Ganesh and M. Widom (unpublished).